Supporting Information

Synthesis, structure and electronic transport properties of phenanthrenone derivatives

Shan-Shan Shen,[a] Ya-Ting Xiao,[a] Zhe-Hao Bai,[a] Zi-Yang Gan,[a] Ye-Hao Ding,[a] Jian-Feng Yan,*[,a] Yuan-Ming Li,*[,a] Yan-Hou Geng,*[,b] and Yao-Feng Yuan*[,a]

([a] *Key Laboratory of Molecule Synthesis and Function Discovery (Fujian Province University), Department of Chemistry, Fuzhou University, Fuzhou 350108, China*)

([b]*Joint School of National University of Singapore and Tianjin University, International Campus of Tianjin University, Fuzhou 350207, China*)

Email: yanjianfeng@fzu.edu.cn; yuanming.li@fzu.edu.cn; yanhou,geng@tju.edu.cn; yaofeng_yuan@fzu.edu.cn

Experimental Section

Table of Content

1. Synthetic Procedures

1.1 Synthesis of 8,9-Bis(4-(methylthio)phenyl)-4H-cyclopenta[def]phenanthren-4-ol (**2**)

In a nitrogen-purged 50 mL three-neck flask equipped with a magnetic stir bar, compound **1** (50 mg, 0.11 mmol, 1 equiv.) was dissolved in dichloromethane (5 mL) under Schlenk conditions. A methanolic solution of sodium borohydride (8.4 mg, 0.22 mmol, 2 equiv. in 5 mL) was added dropwise via syringe. The reaction mixture was stirred at room temperature for 12 h, then quenched with deionized water (20 mL). The aqueous layer was extracted with dichloromethane (3 × 30 mL), and the combined organic phases were washed sequentially with saturated brine (30 mL) and deionized water (30 mL). After drying over anhydrous Na_2SO_4, the solvent was removed under reduced pressure. Purification by column chromatography (petroleum ether/ethyl acetate = 2/1, *V*/*V*) afforded 2 as a pale yellow solid (46.2 mg, 0.10 mmol, 92% yield). R_f = 0.40 (PE/EA = 2/1, *V*/*V*); m.p. 244.3-247.1 °C. ^{1}H NMR (500 MHz, $CDCl_3$) δ 7.81 (d, *J* = 6.6 Hz, 2H), 7.62 – 7.53 (m, 4H), 7.20 – 7.11 (m, 8H), 6.30 (d, *J* = 7.6 Hz, 1H), 2.50 (s, 6H). ^{13}C NMR (126 MHz, $CDCl_3$) δ 143.9, 136.9, 136.2, 135.8, 135.2, 131.6, 131.6, 128.4, 128.3, 125.9, 125.9, 124.9, 121.8, 77.8, 15.7. HRMS (ESI$^+$) m/z calcd for $C_{29}H_{22}OS_2$+Na^+: 473.1004 $[M+Na]^+$; found: 473.1013.

1.2 Synthesis of 8,9-Bis(4-(methylthio)phenyl)-4H-cyclopenta[def]phenanthrene (**3**)

In a nitrogen-purged 25 mL threaded Schlenk tube equipped with a magnetic stir bar, compound **1** (58 mg, 0.13 mmol) and potassium hydroxide (22 mg, 0.4 mmol) were added sequentially under Schlenk conditions. Hydrazine hydrate (0.1 mL, 3.2 mmol) and diethylene glycol (6 mL) were injected via syringe. The reaction mixture was heated at 170 °C for 24 h, then cooled to 0 °C and acidified with concentrated HCl (5 mL). After dilution with deionized water (20 mL), the aqueous layer was extracted with dichloromethane (3 × 30 mL). The combined organic phases were washed with saturated brine (30 mL) and deionized water (30 mL), dried over anhydrous Na_2SO_4, and concentrated under reduced pressure. Purification by column chromatography (PE/DCM = 5/1, *V*/*V*) afforded 3 as a white solid (31 mg, 0.07 mmol, 55% yield). R_f = 0.32 (PE/DCM = 5/1, *V*/*V*); m.p. 256.3-259.1 °C. ^{1}H NMR (500 MHz, $CDCl_3$) δ 7.75

– 7.69 (m, 2H), 7.59 (dd, *J* = 8.1, 6.9 Hz, 2H), 7.54 (d, *J* = 7.7 Hz, 2H), 7.18 (d, *J* = 0.8 Hz, 8H), 4.42 (s, 2H), 2.51 (s, 6H). ^{13}C NMR (126 MHz, $CDCl_3$) δ 141.6, 137.9, 136.7, 136.1, 135.7, 131.7, 128.5, 127.6, 125.9, 122.6, 121.5, 37.6, 15.8. HRMS (ESI$^+$) m/z calcd for $C_{29}H_{22}S_2$+H^+: 435.1237 $[M+H]^+$; found: 435.1236.

1.3 Synthesis of 9,10-Bis(4-(methylthio)phenyl)phenanthrene (**4**)

In a nitrogen-purged 100 mL three-neck flask equipped with a magnetic stir bar, 9,10-dibromophenanthrene (200 mg, 0.60 mmol), 4-(methylthio)phenylboronic acid (300 mg, 1.79 mmol), tetrakis(triphenylphosphine)palladium (34.3 mg, 0.03 mmol), and sodium hydroxide (32 mg, 0.79 mmol) were added sequentially under Schlenk conditions. A solvent mixture of toluene/ethanol/water (4/1/2, *V*/*V*/*V*, 20 mL/5 mL/10 mL) was injected via syringe. The reaction mixture was heated at 85 °C for 48 h, then cooled to room temperature. The aqueous layer was extracted with dichloromethane (3 × 30 mL), and the combined organic phases were washed with saturated brine (30 mL) and deionized water (30 mL). After drying over anhydrous Na_2SO_4, the solvent was removed under reduced pressure. Purification by column chromatography (petroleum ether/dichloromethane = 10/1, *V*/*V*) afforded **4** as a white solid (163.4 mg, 0.39 mmol, 65% yield). R_f = 0.30 (PE/DCM = 5/1, *V*/*V*); m.p. 258.3-261.7 °C. ^{1}H NMR (500 MHz, $CDCl_3$) δ 8.80 (dt, *J* = 8.3, 0.8 Hz, 2H), 7.67 (ddd, *J* = 8.3, 6.8, 1.4 Hz, 2H), 7.55 (dd, *J* = 8.3, 1.4 Hz, 2H), 7.49 (ddd, *J* = 8.1, 6.8, 1.2 Hz, 2H), 7.17 – 7.04 (m, 8H), 2.49 (s, 6H). ^{13}C NMR (126 MHz, $CDCl_3$) δ 136.8, 136.6, 136.4, 132.0, 131.6, 130.2, 127.9, 126.8, 126.6, 125.8, 122.7, 15.7. HRMS (ESI$^+$) m/z calcd for $C_{28}H_{22}S_2$+Na^+: 445.1055 $[M+Na]^+$; found: 445.1060.

2. NMR Characterization

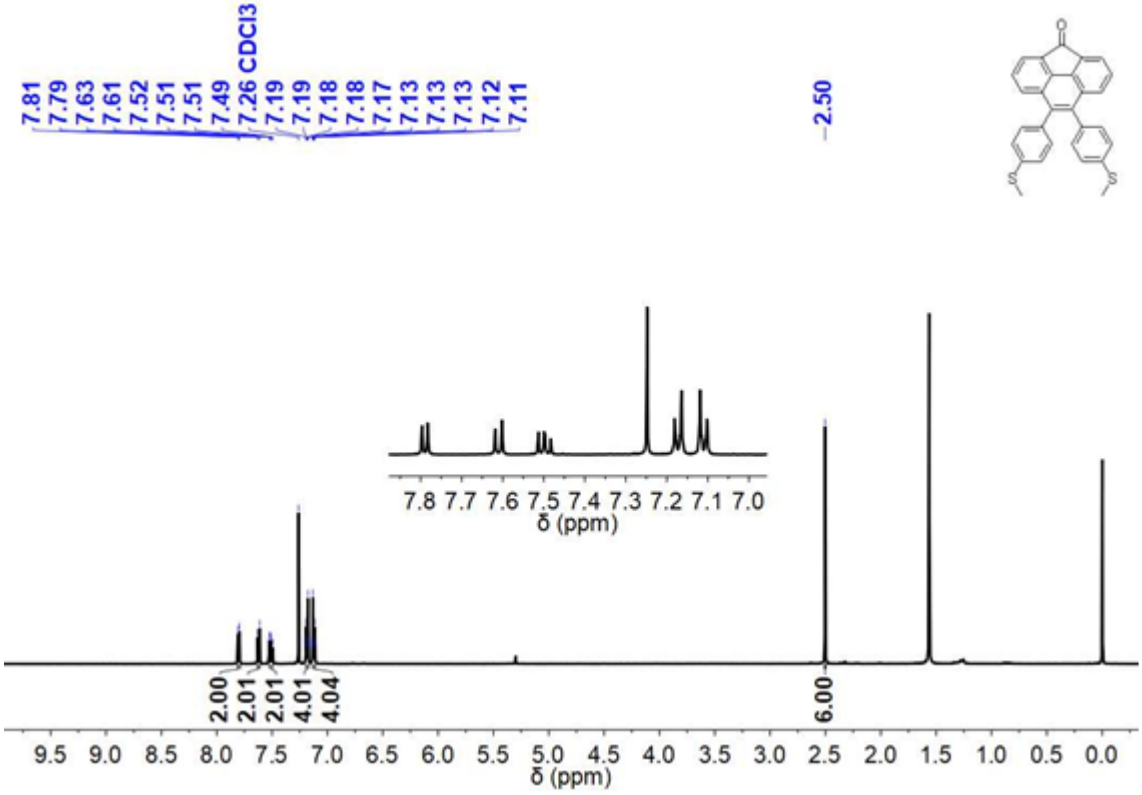

Fig. S1 ^{1}H NMR spectrum of **1** in $CDCl_3$.

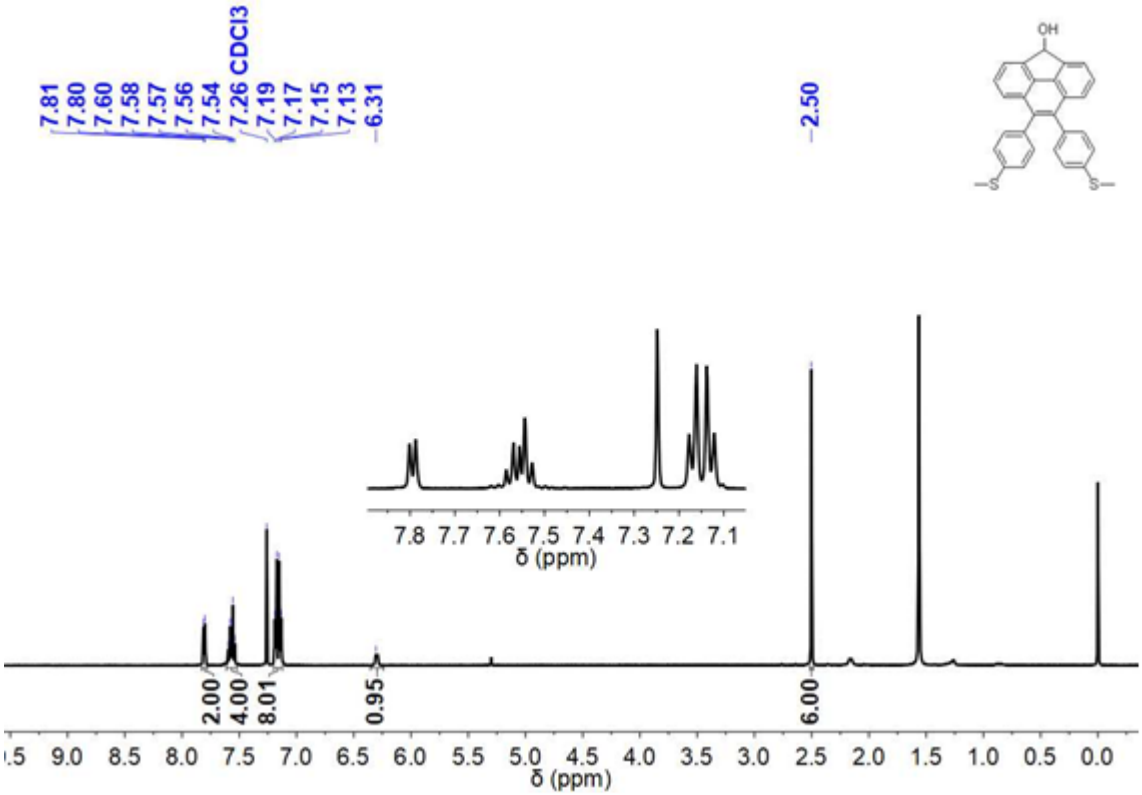

Fig. S2 ^{1}H NMR spectrum of **2** in $CDCl_3$.

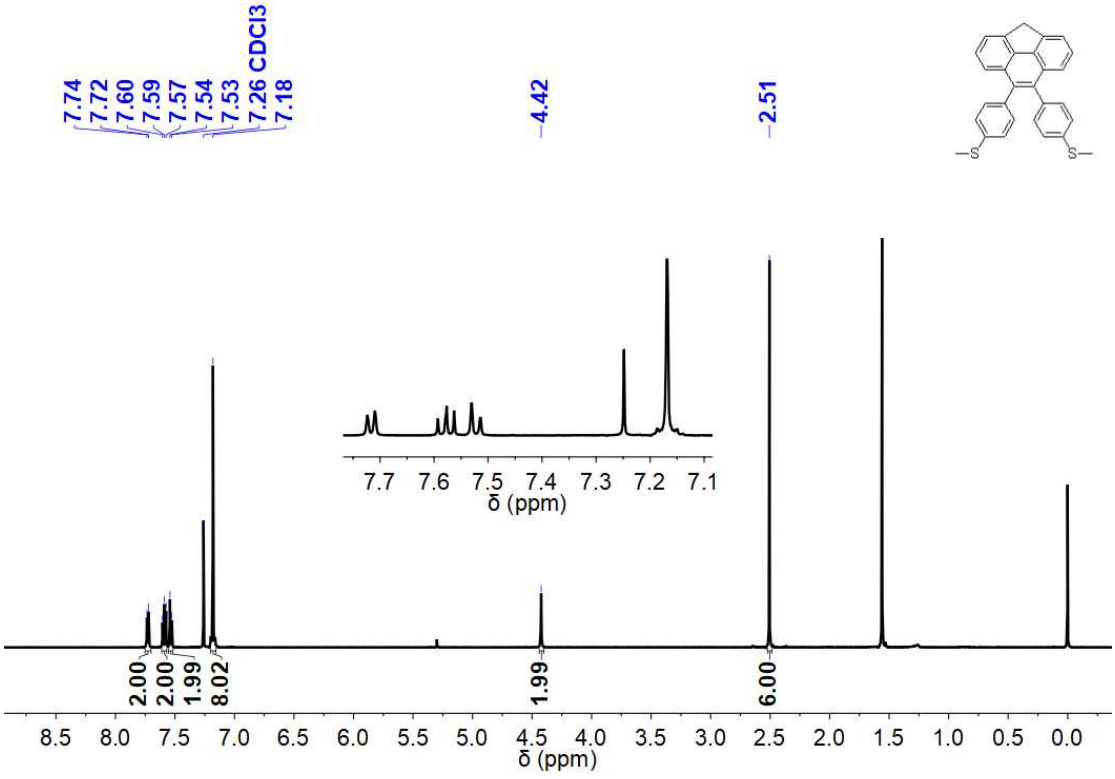

Fig. S3 ^{1}H NMR spectrum of **3** in $CDCl_3$.

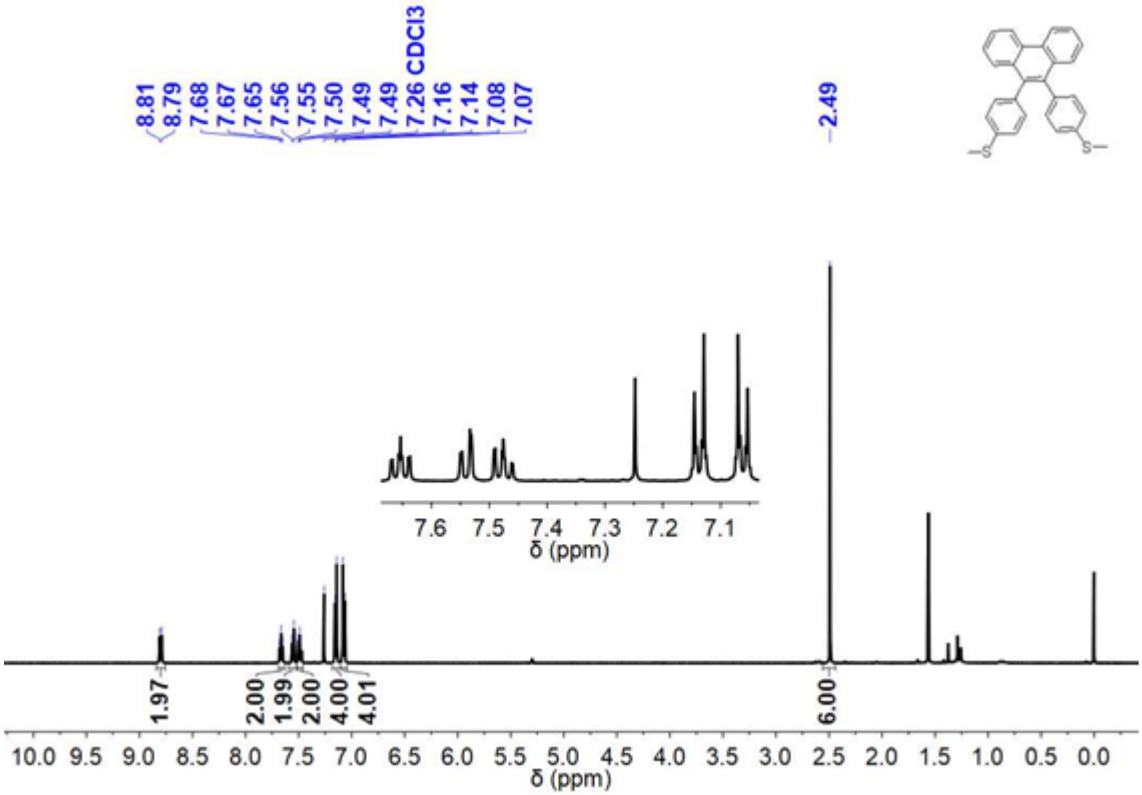

Fig. S4 ^{1}H NMR spectrum of **4** in $CDCl_3$.

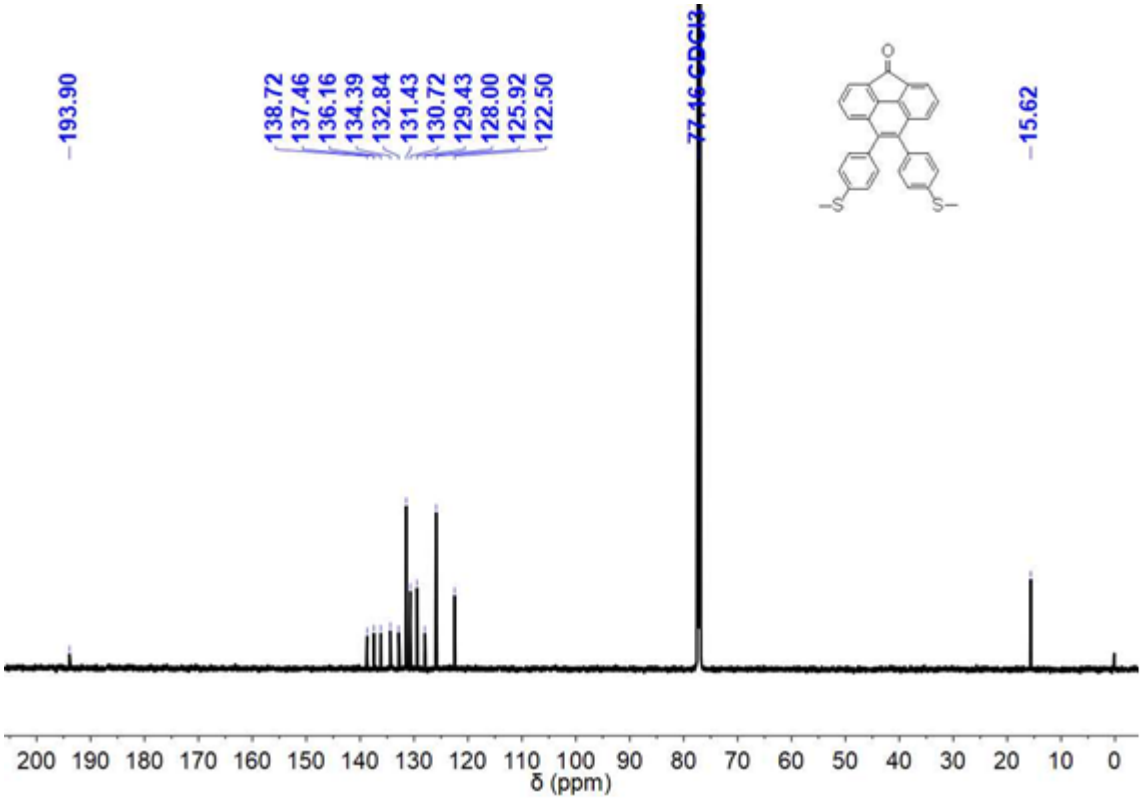

Fig. S5 ^{13}C NMR spectrum of **1** in $CDCl_3$.

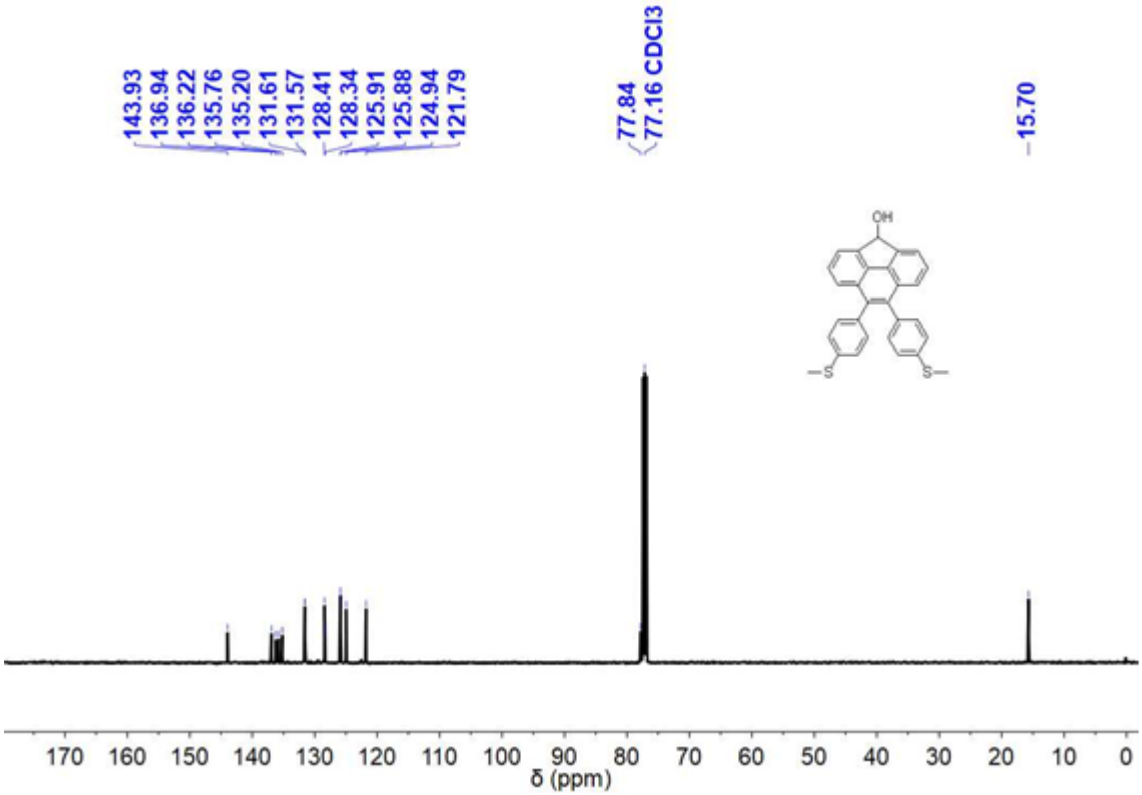

Fig. S6 ^{13}C NMR spectrum of **2** in $CDCl_3$.

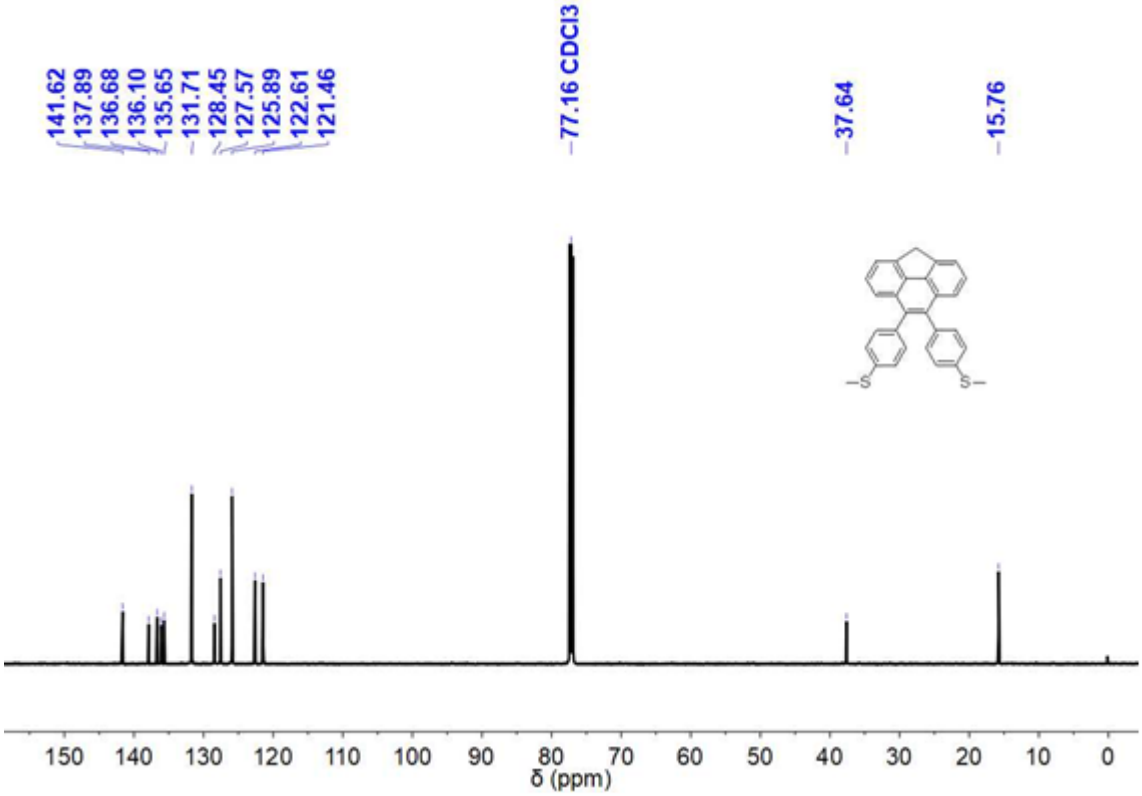

Fig. S7 ^{13}C NMR spectrum of **3** in $CDCl_3$.

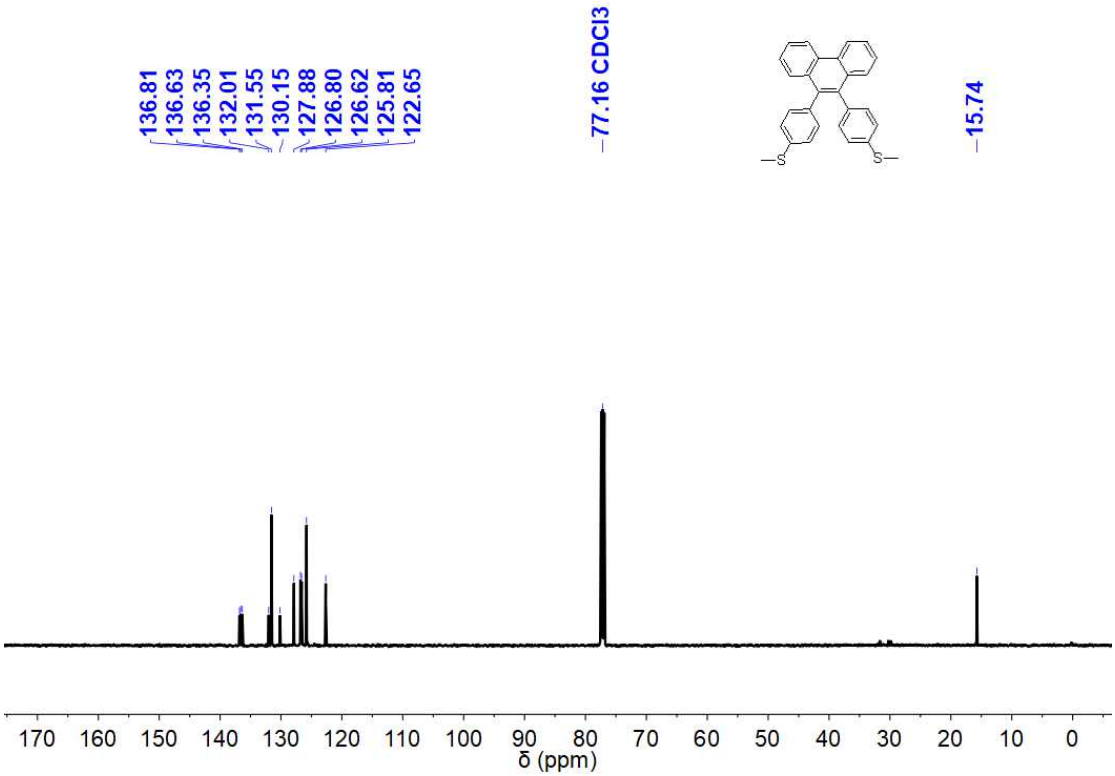

Fig. S8 ^{13}C NMR spectrum of **4** in $CDCl_3$.

3. HRMS Characterization

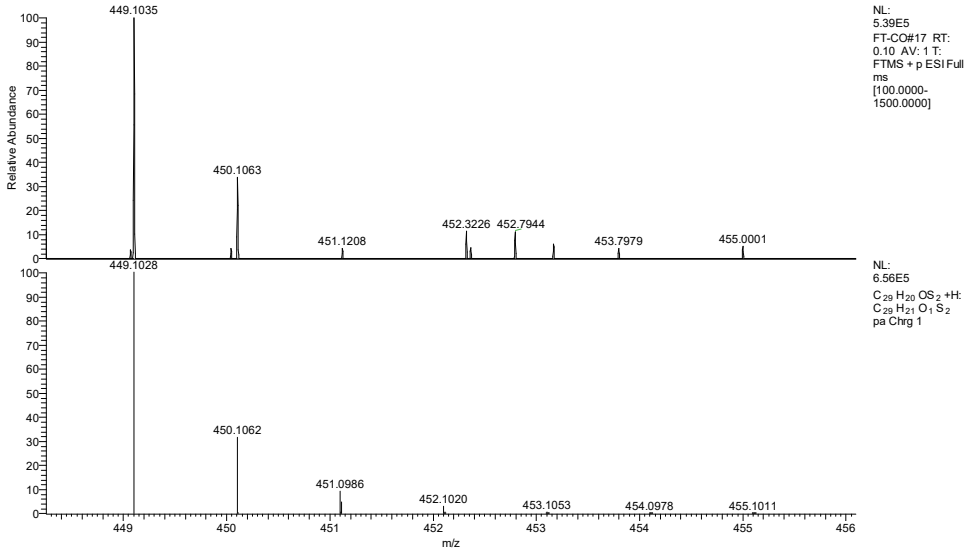

Fig. S9 HRMS of **1**.

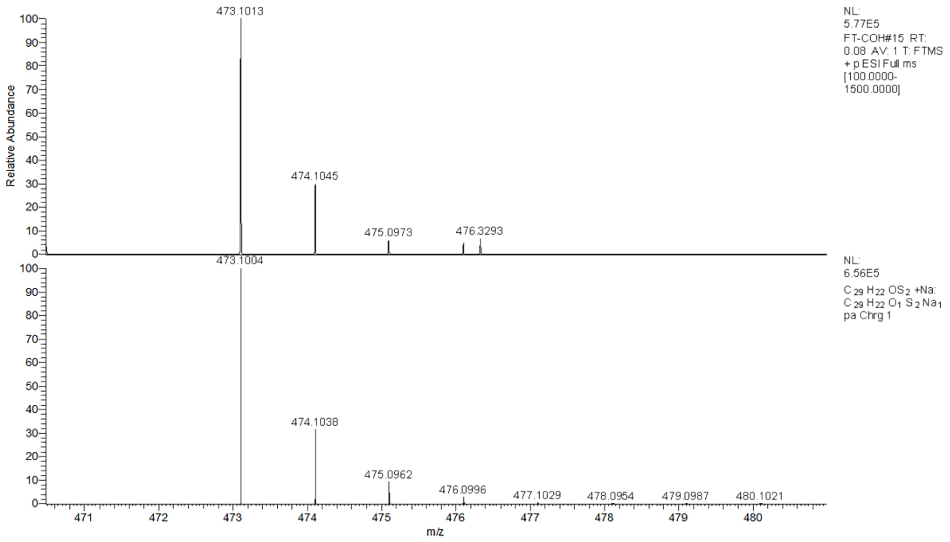

Fig. S10 HRMS of **2**.

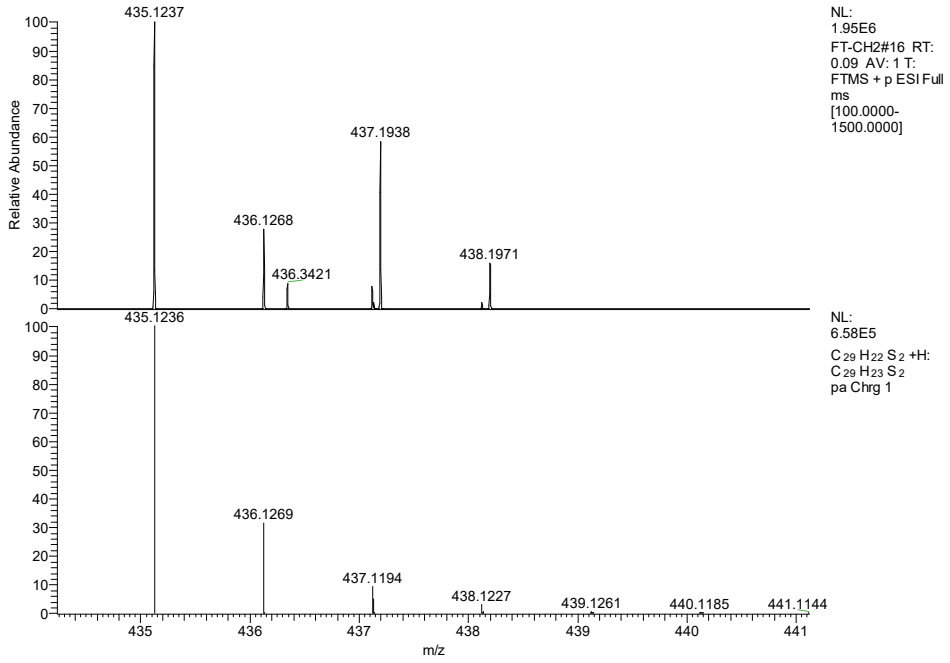

Fig. S11 HRMS of **3**.

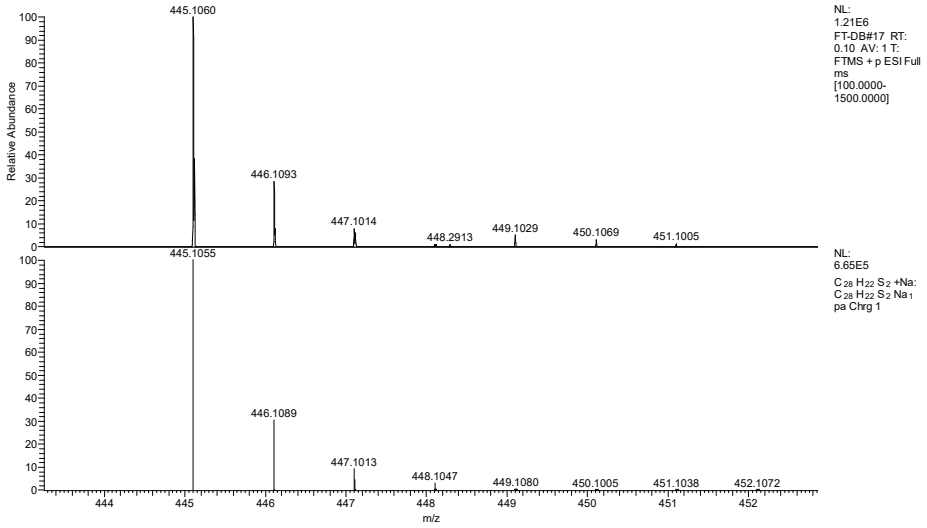

Fig. S12 HRMS of **4**.

4. Crystal data

Table S1. Crystallographic data and collection parameters for **1, 2, 3** and **4**.

Compound	**1**	**2**	**3**	**4**
CCDC number	2367744	2367745	2371231	2371119
Empirical formula	$C_{29}H_{20}OS_2$	$C_{29}H_{22}OS_2$	$C_{29}H_{22}S_2$	$C_{28}H_{22}S_2$
Formula weight	44857	450.58	434.58	422.57
Temperature/K	296.15	296.15	296.15	296.15
Crystal system	triclinic	triclinic	triclinic	monoclinic
Space group	$P\bar{1}$	$P\bar{1}$	$P\bar{1}$	$P2_1/c$
a/Å	10.1764(6)	10.2519(8)	10.2762(5)	16.7680(9)
b/Å	11.0252(9)	10.7695(6)	11.0227(4)	7.8383(3)
c/Å	11.7176(8)	12.0148(6)	11.6637(6)	17.1786(10)
α/°	66.231(7)	66.426(5)	65.358(4)	90
β/°	86.740(5)	85.195(5)	84.730(4)	109.761(6)
γ/°	63.175(7)	64.595(7)	63.792(4)	90

Volume/Å^3	1061.04(15)	1092.05(14)	1061.04(15)	2124.9(2)
Z	2	2	2	4
μ/mm^{-1}	0.272	0.264	0.264	0.263
F(000)	468.0	472.0	456.0	888.0
2θ range / °	3.844 to 71.498	3.72 to 71.228	3.866 to 71.044	4.172 to 52.744
Reflections collected	36458	39858	23833	34508
Independent reflections	6931	7241	6575	4339
Data/restraints/parameters	6931/0/291	7241/0/297	6575/0/290	4339/0/273
Goodness−of−fit on F^2	1.037	1.037	1.038	1.063
Final R indices	R_1 = 0.0600	R_1 = 0.0631	R_1 = 0.0635	R_1= 0.0483
	wR_2= 0.1107	wR_2= 0.1272	wR_2=0.1246	wR_2 = 0.1077
R indices	R_1 = 0.1354	R_1 = 0.1424	R_1 = 0.1294	R_1= 0.0806
	wR_2 = 0.1376	wR_2= 0.1558	wR_2 = 0.1568	wR_2 = 0.1208

5. Cyclic voltammetry

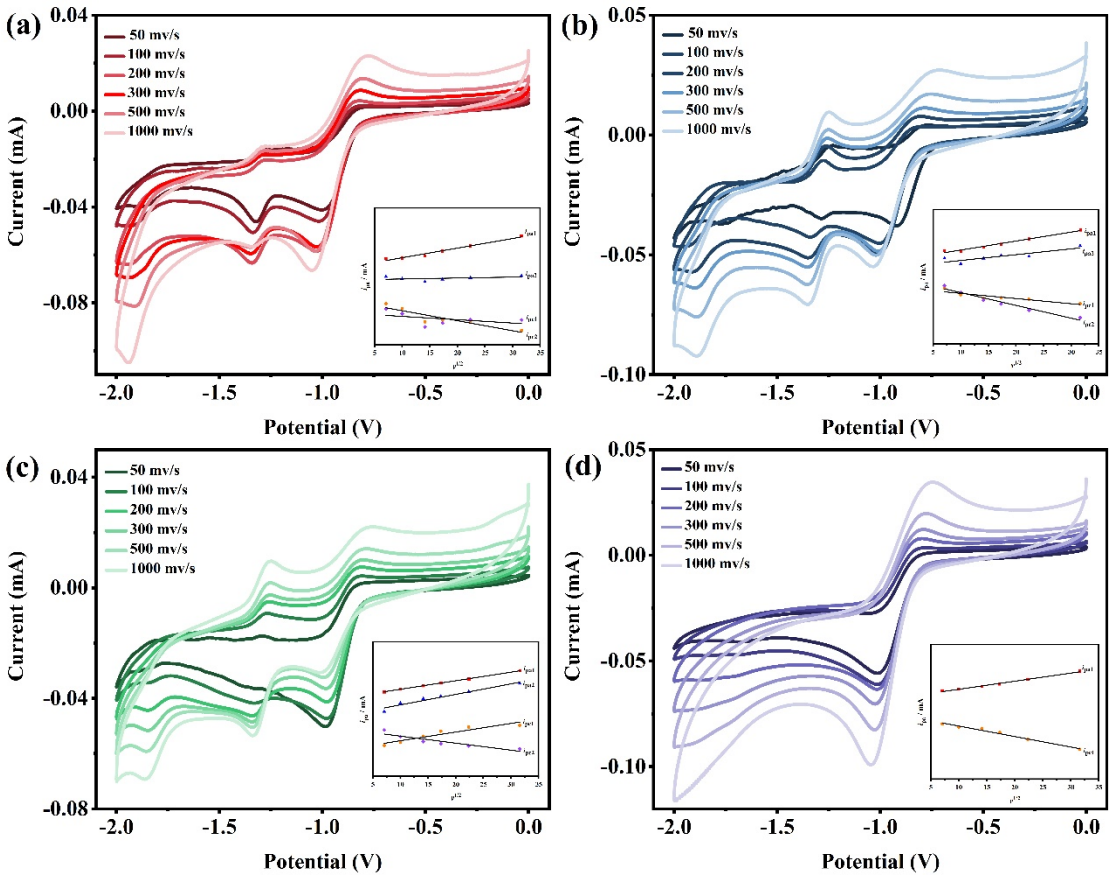

Fig. S13. Cyclic voltammograms of **1**(a), **2**(b), **3**(c), and **4**(d) (1.0×10^{-3} mol L^{-1}) in 0.1 mol L^{-1} $TBAPF_6$ and CH_2Cl_2/CH_3CN (1/1, *V*/*V*) solution. Scan rates were 50, 100, 200, 300, 500, and 1000 mV s^{-1}, respectively. The inset shows the linear relationship between the peak current and the square root of the scan rate for the corresponding molecules.

Table S2. Electrochemical data for **1-4** at a scan rate of 100 mV·s^{-1}.

Compound		E_{pa}/V	i_{pa}/mA	E_{pc}/V	i_{pc}/mA	ΔE_p/V
1	1	−0.816	0.002	−1.019	−0.046	0.203
	2	−1.271	0.017	−1.337	−0.051	0.066
2	1	−0.809	0.004	−1.008	−0.045	0.199
	2	−1.273	−0.011	−1.342	−0.043	0.069
3	1	−0.807	0.004	−0.981	−0.047	0.174

	2	−1.269	−0.009	−1.331	−0.042	0.062
4	/	−0.782	0.004	−1.011	−0.061	0.229

6. Theoretical Calculations

6.1 Frontier Molecular Orbitals

Table S3. Frontier Orbital Energy Levels of **1**, **2**, **3**, and **4.**

	1	**2**	**3**	**4**
HOMO/eV	−5.87	−5.70	−5.58	−5.29
LUMO/eV	−2.33	−1.50	−1.40	−1.11
Gap/eV	3.54	4.20	4.18	4.18

Table S4. Atomic coordinates of **1** after geometry optimization.

Atom	X/Å	Y/Å	Z/Å
C	−7.3673	1.9858	0.7424
C	−6.0528	1.7711	0.5100
C	−5.3427	2.8722	0.7435
C	−5.7680	4.0875	1.0874
C	−7.0797	4.2830	1.2507
C	−7.8598	3.1982	1.0807
C	−5.3395	0.6564	0.1898
C	−3.9644	0.6885	0.1389
C	−3.2835	1.8429	0.3788
C	−4.0244	2.9067	0.6796
C	−1.9767	2.1761	0.2817
C	−1.5192	3.4195	0.5496
C	−2.3292	4.4375	0.8984
C	−3.6342	4.1534	0.9433
C	−4.7127	4.9362	1.2166
C	−6.0286	−0.5044	0.0472
C	−3.2435	−0.3865	−0.2701
C	−7.1539	−0.5800	−0.6931
C	−7.8333	−1.7275	−0.8472
C	−7.3989	−2.8475	−0.2528
C	−6.2811	−2.8067	0.4854
C	−5.6128	−1.6510	0.6260
C	−3.6322	−1.1432	−1.3184

C	−3.6322	−2.2132	−1.7268
C	−2.9321	−2.5627	−1.0848
C	−1.4008	−1.8363	−0.0348
C	−2.118	−0.7675	0.3578
S	−8.3031	−4.4160	−0.4467
S	−0.8616	−4.0165	−1.6367
C	−9.7187	−3.9648	0.5958
C	0.5376	−3.0950	−2.3349
O	−4.7294	6.1102	1.5063
H	−8.1057	1.1709	0.6976
H	−7.4936	5.2611	1.5402
H	−8.9454	3.3057	1.2520
H	−1.2164	1.4540	−0.0526
H	−0.4380	3.6233	0.4553
H	−1.9437	5.4487	1.0999
H	−7.5222	0.2946	−1.2565
H	−8.7354	−1.7442	−1.4813
H	−5.9109	−3.7145	0.99905
H	−4.7247	−1.6702	1.2803
H	−4.5237	−0.8797	−1.9125
H	−3.2811	−2.7916	−2.5986
H	−0.4945	−2.1218	0.5249
H	−1.7634	−0.2457	1.2657
H	10.4131	−4.8322	0.6589
H	9.3731	−3.7064	1.6218
H	−10.2679	−3.1007	0.1602
H	1.2546	−3.8146	−2.7895
H	0.1814	−2.3962	−3.1246
H	1.0653	−2.5209	−1.5413

Table S5. Atomic coordinates of **2** after geometry optimization.

Atom	X/Å	Y/Å	Z/Å
C	5.0201	−13.8481	−0.3289
C	5.1604	−12.5204	−0.5367
C	4.0612	−11.9701	−1.057
C	2.9405	−12.5919	−1.4354
C	2.8585	−13.9149	−1.2629
C	3.9128	−14.5254	−0.6951

C	6.1747	−11.675	−0.2122
C	6.0473	−10.3215	−0.4046
C	4.9119	−9.8008	−0.9418
C	3.9407	−10.6634	−1.2488
C	4.6174	−8.5390	−1.3253
C	3.4315	−8.2076	−1.8756
C	2.474	−9.1212	−2.1105
C	2.7536	−10.3907	−1.7988
C	1.9100	−11.6301	−1.976
C	7.2657	−12.1909	0.4091
C	7.0892	−9.4833	−0.1721
C	7.9027	−13.2861	−0.0544
C	9.0103	−13.7674	0.5324
C	9.5128	−13.1596	1.6164
C	8.8933	−12.0787	2.1101
C	7.7892	−11.6093	1.5092
C	8.3438	−9.7961	−0.5601
C	9.3927	−9.0009	−0.2991
C	9.2098	−7.8537	0.3691
C	7.9738	−7.5089	0.757
C	6.9352	−8.3149	0.4847
S	11.0304	−13.794	2.3973
S	10.6232	−6.7751	0.7617
C	12.0999	−12.4127	1.9001
C	11.3866	−7.8846	1.9804
O	0.7944	−11.5804	−1.1023
H	5.7901	−14.4448	0.183
H	1.9472	−14.4658	−1.5422
H	3.8521	−15.6103	−0.4998

H	5.3433	−7.7165	−1.2383
H	3.2433	−7.1593	−2.1664
H	1.5109	−8.8512	−2.5700
H	1.5969	−11.8292	−3.0204
H	7.5753	−13.7816	−0.9847
H	9.5180	−14.6455	0.0992
H	9.2797	−11.5704	3.0093
H	7.3043	−10.7362	1.9782
H	8.5498	−10.7115	−1.1405
H	10.3979	−9.2988	−0.6412
H	7.8064	−6.5792	1.3263
H	5.9527	−8.0176	0.8904
H	13.1406	−12.6214	2.2346
H	12.0946	−12.3013	0.7926
H	11.7610	−11.4621	2.3685
H	12.2774	−7.3826	2.4194
H	10.6655	−8.1140	2.7967
H	11.7152	−8.8330	1.5003
H	1.1689	−11.4142	−0.2332

Table S6. Atomic coordinates of **3** after geometry optimization.

Atom	X/Å	Y/Å	Z/Å
C	4.6642	−13.4786	−0.3374
C	4.8000	−12.1512	−0.5502
C	3.6993	−11.6063	−1.0736
C	2.579	−12.2323	−1.4491
C	2.5041	−13.5559	−1.2738
C	3.5597	−14.1609	−0.7025

C	5.8117	−11.3018	−0.2284
C	5.6803	−9.9494	−0.4251
C	4.5434	−9.4339	−0.9641
C	3.5748	−10.3004	−1.2697
C	4.2458	−8.1739	−1.3509
C	3.0597	−7.8477	−1.9037
C	2.1054	−8.765	−2.1374
C	2.3856	−10.0333	−1.8195
C	1.5479	−11.278	−2.0085
C	6.9038	−11.8123	0.3953
C	6.7196	−9.1075	−0.1945
C	7.5447	−12.9068	−0.0645
C	8.6534	−13.3827	0.5245
C	9.1532	−12.7701	1.6070
C	8.5298	−11.6897	2.0971
C	7.4246	−11.2257	1.4941
C	7.9753	−9.4177	−0.5814
C	9.0219	−8.6191	−0.3219
C	8.8355	−7.4709	0.3436
C	7.5985	−7.1286	0.7303
C	6.5621	−7.9380	0.4594
S	10.6725	−13.3974	2.3903
S	10.246	−6.388	0.7347
C	11.7353	−12.0086	1.8997
C	11.0088	−7.4922	1.9586
H	5.4361	−14.0709	0.1768
H	1.5971	−14.1121	−1.5564
H	3.5034	−15.2457	−0.5056
H	4.9695	−7.3492	−1.2661

H	2.8696	−6.8013	−2.1998
H	1.1442	−8.4992	−2.6035
H	0.6231	−11.2548	−1.3903
H	1.3355	−11.4779	−3.0823
H	7.2194	−13.406	−0.9935
H	9.1643	−14.2604	0.0942
H	8.9138	−11.1775	2.9951
H	6.9367	−10.3526	1.9600
H	8.1840	−10.3341	−1.1594
H	10.0281	−8.915	−0.6627
H	7.4285	−6.1982	1.2976
H	5.5788	−7.6425	0.8642
H	12.7767	−12.2134	2.2344
H	11.7306	−11.8927	0.7927
H	11.3913	−11.0616	2.3717
H	11.8984	−6.9876	2.3973
H	10.2867	−7.7197	2.7745
H	11.3392	−8.4419	1.4824

Table S7. Atomic coordinates of **4** after geometry optimization.

Atom	X/Å	Y/Å	Z/Å
C	6.2945	−6.4994	0.1207
C	7.1	−7.5863	0.1017
C	8.4207	−7.3936	0.3354
C	8.8638	−6.1206	0.4501
C	8.0582	−5.052	0.396
C	6.7464	−5.2457	0.2495
C	9.2455	−8.4625	0.4525

C	8.7415	−9.7151	0.3397
C	9.617	−10.7467	0.3375
C	10.9315	−10.6013	0.5456
C	11.4152	−9.3729	0.7384
C	10.5734	−8.333	0.6753
C	6.5967	−8.839	−0.0326
C	7.4166	−9.9103	0.1241
C	5.2656	−9.0211	−0.2297
C	6.9284	−11.1681	−0.0254
C	7.1497	−12.1232	0.9023
C	6.6312	−13.3562	0.7884
C	5.8704	−13.6664	−0.2708
C	5.6406	−12.7404	−1.2123
C	6.1631	−11.5111	−1.0825
C	4.5403	−9.8609	0.5384
C	3.2318	−10.07	0.3248
C	2.6091	−9.4367	−0.6791
C	3.3047	−8.5999	−1.4622
C	4.6125	−8.4002	−1.2346
S	0.8353	−9.7279	−0.9695
S	5.1491	−15.332	−0.4164
C	0.2668	−8.098	−0.4085
C	3.4444	−14.8351	−0.0349
H	5.1971	−6.5579	0.0636
H	9.9154	−5.8479	0.6147
H	8.4573	−4.0297	0.5094
H	6.0542	−4.3869	0.254
H	9.325	−11.7879	0.1331
H	11.6099	−11.4711	0.5413

H	12.4953	−9.2239	0.9071
H	11.0837	−7.369	0.8071
H	7.7204	−11.8962	1.8202
H	6.8158	−14.0995	1.5819
H	5.0268	−12.9789	−2.0969
H	5.9668	−10.7937	−1.8977
H	4.9962	−10.3802	1.3986
H	2.6762	−10.7575	0.9844
H	2.8165	−8.0872	−2.3077
H	5.1547	−7.7447	−1.939
H	−0.8447	−8.066	−0.456
H	0.5863	−7.9209	0.6429
H	0.6731	−7.2935	−1.0608
H	2.7968	−15.7401	−0.0229
H	3.4008	−14.3492	0.9656
H	3.0578	−14.1311	−0.8049

6.2 TD-DFT Calculations

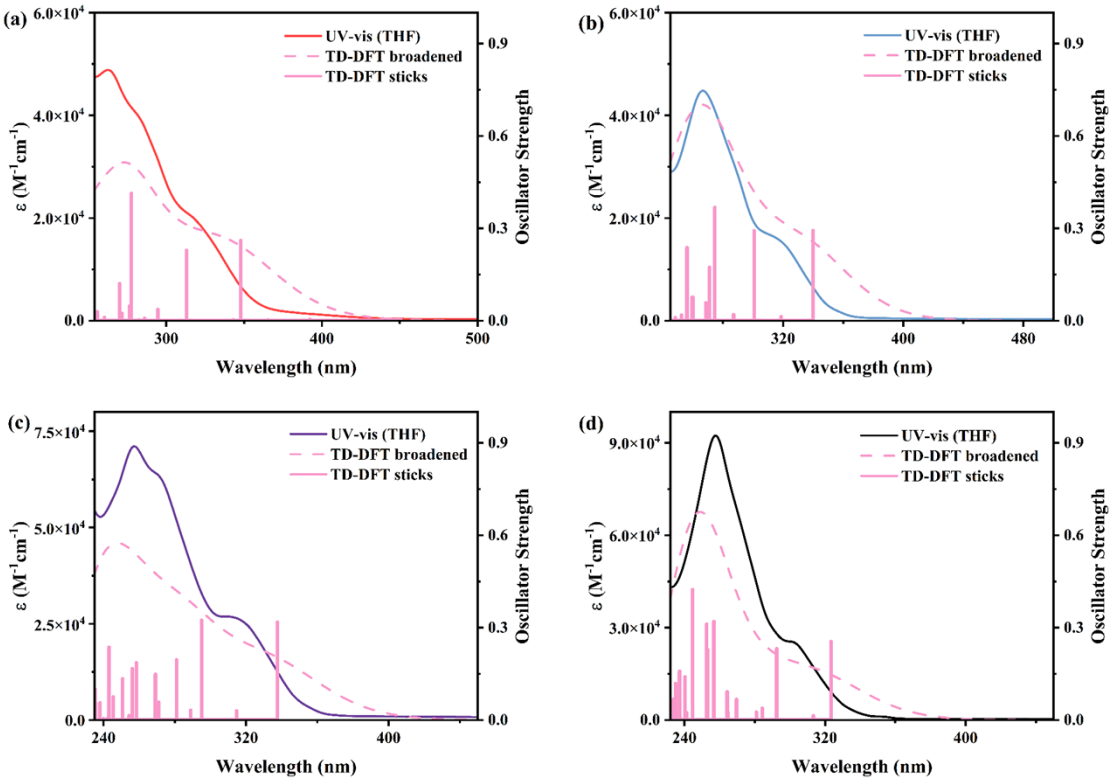

Fig. S14. (a) Experimental UV-Vis spectrum (red curve) and calculated TD-DFT spectrum (pink curve) for **1**; (b) Experimental UV-Vis spectrum (blue curve) and calculated TD-DFT spectrum (pink curve) for **2**; (c) Experimental UV-Vis spectrum (green curve) and calculated TD-DFT spectrum (pink curve) for **3**; (d) Experimental UV-Vis spectrum (purple curve) and calculated TD-DFT spectrum (pink curve) for **4**.

Table S8. Major electronic transitions for **1** by TD-DFT method using CAM-B3LYP/6 31G(d).

1	Energy /eV	Excitation /nm	Qscillator strength/*f*	Description
S4	4.10	302	0.45650	H→L+1(86.3%); H−3→L+1(6.4%).
S9	4.87	254	0.89810	H−1→L+1(57.6%);H→L+2(15.4%).
S13	5.23	237	0.36890	H→L+2(33.8%);H−2→L+1(27.0%);H→L+6(11.3%);H−1→L+1(8.4%).
S14	5.42	228	0.13450	H→L+3(35.1%);H→L+5(22.3%); H−1→L+4(9.5%);H−1→L+2(7.8%).
S16	5.67	218	1.10780	H−2→L+2(46.3%);H−7→L(16.4%);H−1→L+2(14.5%);H−5→L(5.1%).

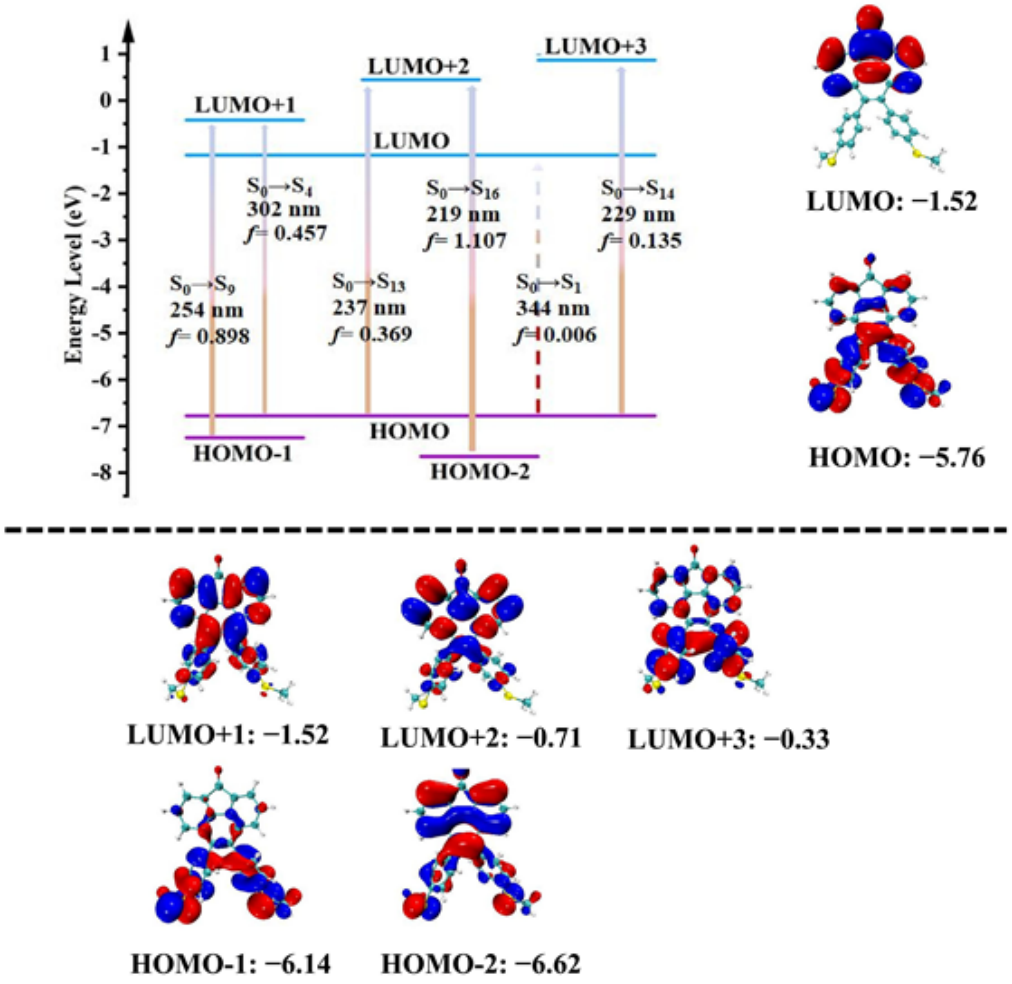

Fig. S15 Energy level distribution and main transitions of **1**.

Table S9. Major electronic transitions for **2** by TD-DFT method using CAM-B3LYP/6 31G(d).

2	Energy/eV	Excitation/nm	Qscillator strength/*f*	Description
S1	4.12	301	0.44230	H→L(85.8%); H−3→L(5.2%).
S3	4.78	259	0.14940	H−2→L+1(27.4%); H−3→L(27.0%); H−1→L+1(21.0%); H→L+3(10.2%); H→L(5.1%).
S4	4.84	256	0.93500	H−1→L(40.3%); H→L+1(34.8%); H→L+2(7.1%).
S8	5.06	245	0.22860	H−2→L(34.6%); H→L+2(20.5%); H→L+1(11.7%);

				H−1→L(8.0%); H−1→L+3(5.1%).
S9	5.27	235	0.19950	H→L+2(32.0%); H−2→L(27.7%); H→L+4(6.6%); H→L+6(6.1%); H−1→L(5.8%).
S10	5.32	233	0.22200	H−2→L+2(18.9%); H−6→L+1(17.2%); H−1→L+2(14.3%); H−3→L(10.5%); H−2→L+1(7.9%); H−2→L+4(5.8%).
S17	5.95	208	0.26810	H−3→L+3(29.3%); H−2→L+2(13.9%); H−1→L+6(10.1%); H−1→L+2(9.9%); H−3→L+5(9.5%); H→L+3(5.9%).
S19	6.03	206	0.25410	H−4→L(43.7%); H−1→L+1(15.9%); H→L+5(9.6%); H−6→L+1(6.3%); H−2→L+1(6.1%).

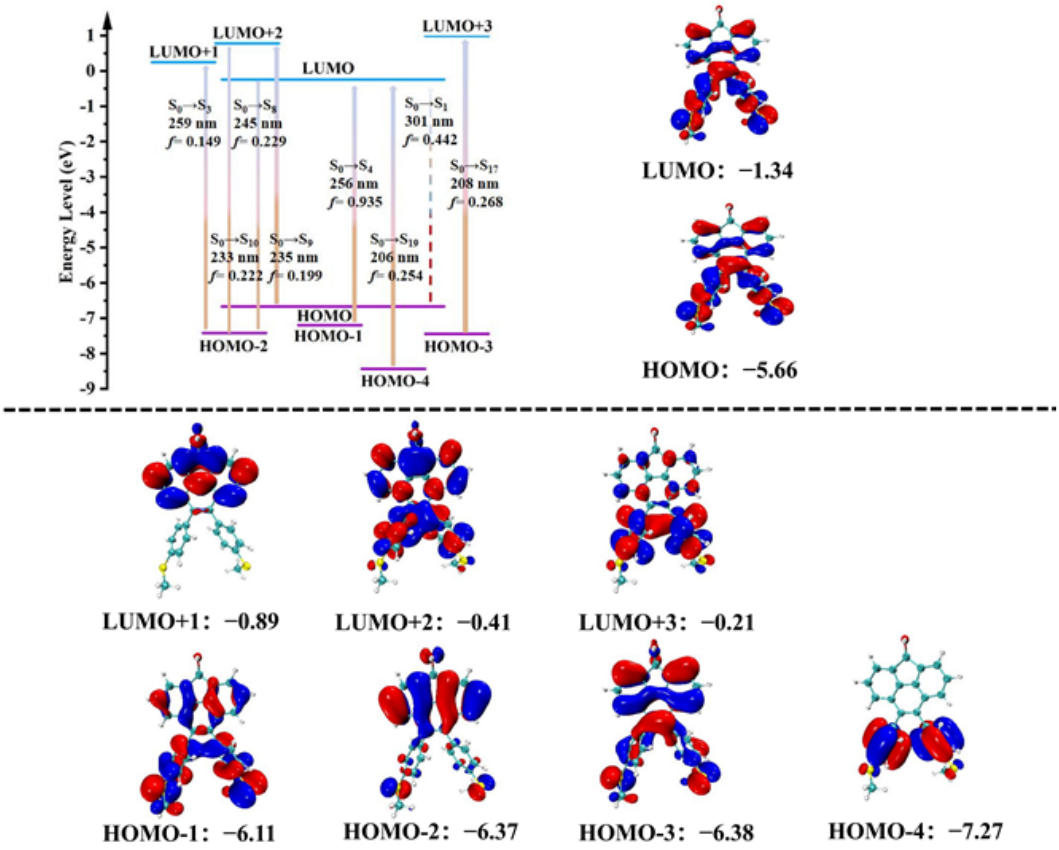

Fig. S16 Energy level distribution and main transitions of **2**.

Table S10. Major electronic transitions for **3** by TD-DFT method using CAM-B3LYP/6 31G(d).

3	Energy/eV	Excitation/nm	Qscillator strength/*f*	Description
S1	4.12	301	0.45910	H→L(86.9%).
S4	4.88	254	1.05460	H→L+1(35.1%); H−1→L(32.9%); H→L+2(13.3%).
S6	5.04	246	0.19700	H→L+4(25.0%); H−1→L(15.6%); H−1→L+3(10.1%); H→L+2(6.9%); H−3→L(6.6%)
S8	5.26	236	0.58900	H−1→L+1(37.8%); H−2→L(25.3%); H−3→L+1(23.0%).
S9	5.30	234	0.14600	H→L+2(39.2%); H−3→L(20.5%); H→L+4(12.7%); H−1→L(5.8%).

S16	5.92	209	0.29190	H−2→L+3(32.4%); H−3→L+2(13.4%); H−1→L+2(10.1%); H−2→L+5(9.6%); H−1→L+6(6.8%); H→L+3(6.0%).
S20	6.11	203	0.10900	H−4→L(66.1%); H−2→L+3(7.9%); H−1→L+1(6.8%); H−3→L+1(6.5%).

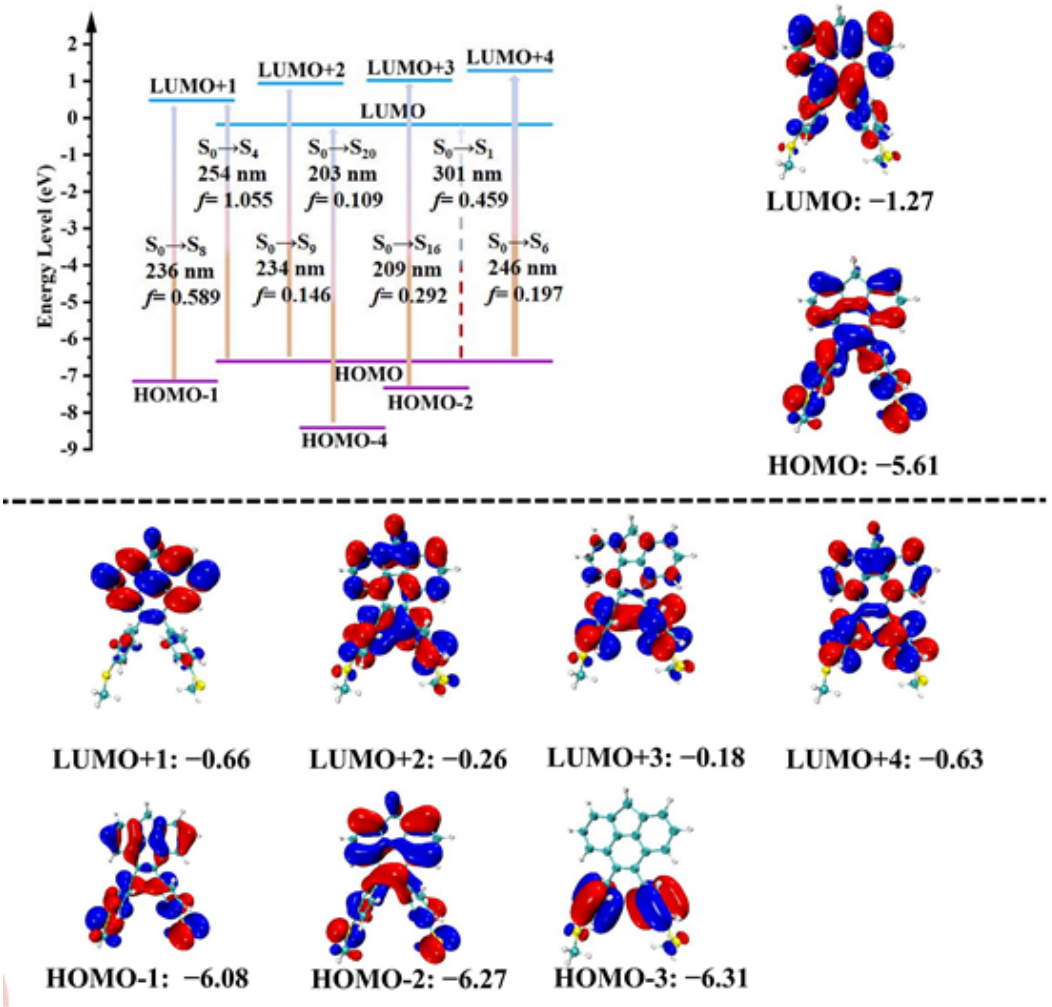

Fig. S17 Energy level distribution and main transitions of **3**.

Table S11. Major electronic transitions for **4** by TD-DFT method using CAM-B3LYP/6 31G(d).

4	Energy/eV	Excitation/nm	Qscillator strength/*f*	Description
S2	4.30	288	0.40390	H→L(78.2%); H−2→L(9.7%); H−3→L+1(6.0%).

S3	4.90	253	0.15520	H−2→L(35.3%); H→L+2(21.3%); H−3→L+1(13.2%); H→L(8.4%).
S4	4.94	251	0.52620	H→L+1(22.8%); H→L+3(20.8%); H−1→L(15.2%); H−3→L(9.2%); H−1→L+5(7.2%); H→L+4(5.7%).
S6	5.08	244	0.50710	H−1→L(35.7%); H→L+4(16.1%); H−1→L+2(9.2%); H→L+3(5.3%); H−2→L+1(5.0%).
S8	5.30	234	0.90140	H−3→L+1(45.3%); H−2→L(33.4%); H−1→L+1(13.8%).
S10	5.43	228	0.26450	H→L+3(33.6%); H→L+4(24.1%); H−1→L(15.3%); H−1→L+2(6.6%); H−3→L(6.2%).
S16	5.86	212	0.19900	H−2→L+2(49.0%); H−1→L+3(8.7%); H→L+2(6.6%); H−1→L+4(6.0%); H−1→L+6(5.5%).

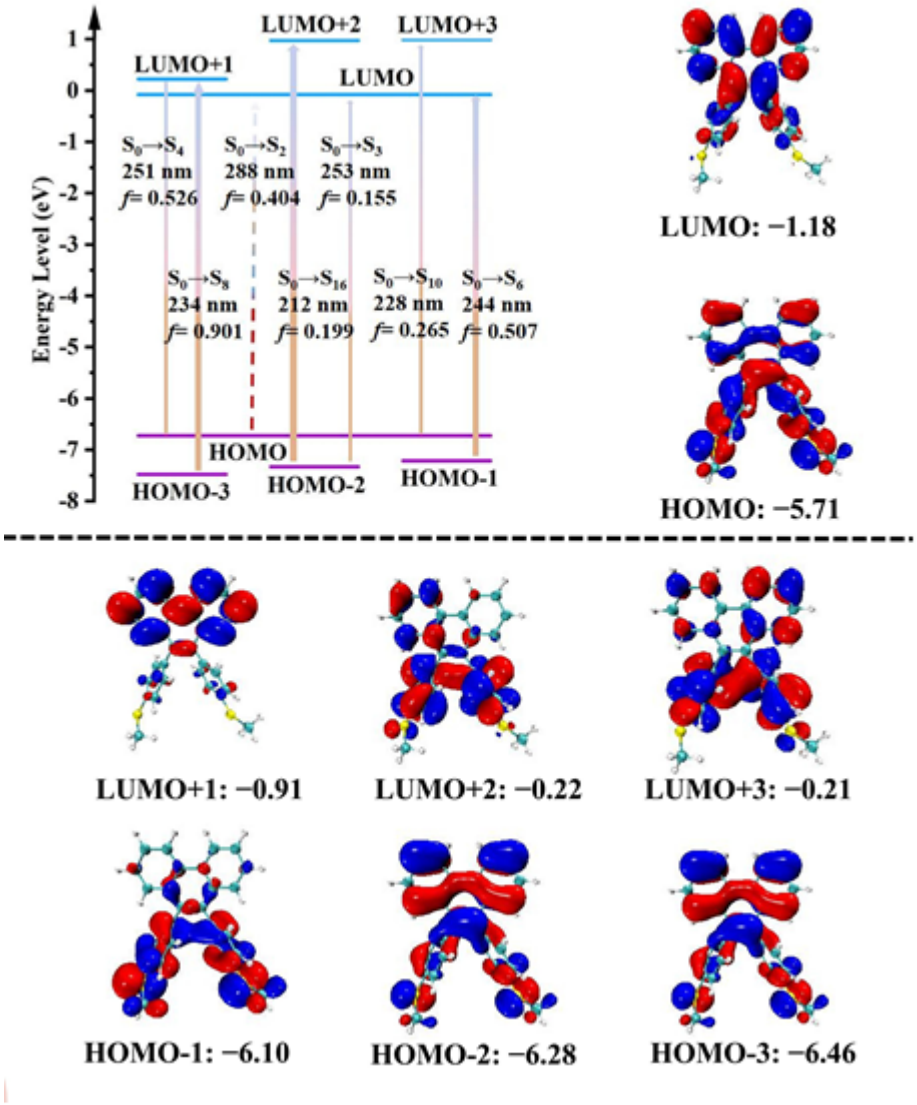

Fig. S18 Energy level distribution and main transitions of **4**.

7. Single-Molecule Conductance Test

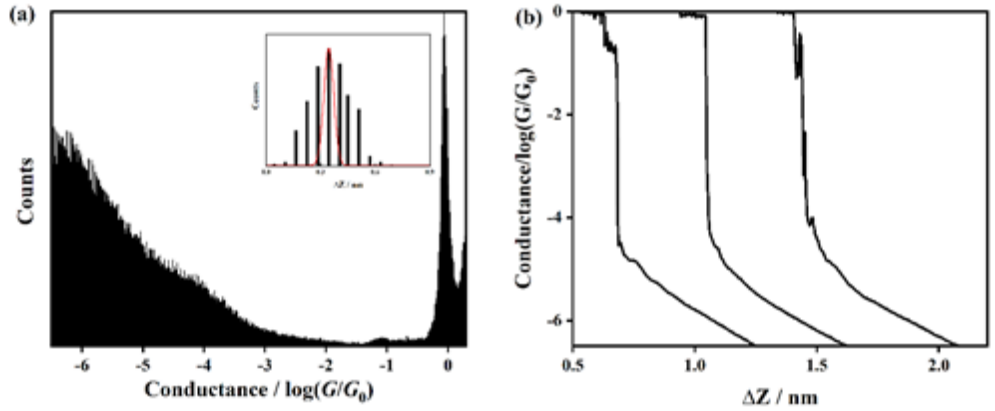

Fig. S19 (a) One-dimensional conductance histogram and molecular junction length distribution (Inset) during pure solvent correction; (b) Single trace plot during pure solvent correction.